SEMARAK ILMU PUBLISHING

Journal of Advanced Research in Fluid Mechanics and Thermal Sciences

Journal homepage:
https://semarakilmu.com.my/journals/index.php/fluid_mechanics_thermal_sciences/index
ISSN: 2289-7879

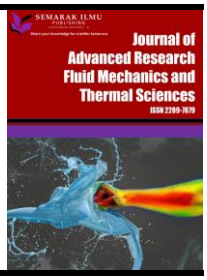

Advanced Natural Circulation Model in Evaporation Circuits of Thermosiphon Waste Heat Boilers

Dolganov Iurii[1,*], Epifanov Alexander[2], Lychko Bohdan[3]

[1] Faculty of Science, Technology and Medicine, Department of Engineering, University of Luxembourg, L-1359, Luxembourg
[2] Department of Thermal Physics and Steam-Generating Units, Admiral Makarov National University of Shipbuilding, Mykolaiv, Ukraine
[3] Department of Operation of Marine Stationary Power Plants, Admiral Makarov National University of Shipbuilding, Mykolaiv, Ukraine

ARTICLE INFO

Article history:
Received 28 August 2023
Received in revised form 19 November 2023
Accepted 27 November 2023
Available online 15 December 2023

Keywords:
Thermosiphon; waste heat boiler; natural circulation; cogeneration power plant; numerical simulation

ABSTRACT

Although existing models of natural circulation in steam boilers involve numerous simplifications, the physical processes that occur in real-time are not considered. This study sought to improve the natural circulation model in the evaporation circuit of a thermosiphon waste heat boiler using an analytical solution and numerical simulation results. A modified natural circulation model was developed using ranked variables of velocity and heat flux in the evaporator ring channels. These results were obtained in the range of heat flux densities 1.074–9.973 kW/m^2 and temperatures of the thermosiphons hot zone 477.4–487.1 K which is typical for a waste heat boiler for cogeneration power plant with gas turbine engine 6700 kW power.

1. Introduction

1.1 Research Background

Heat pipes and gravity thermosiphons are known to be efficient and reliable for heat transfer [1,2]. Therefore, using them as heat exchange surfaces in waste heat boilers (WHBs), economizers, and air heaters in power plants can increase the efficiency of conversion of primary energy carriers, energy security of the system, and sustainability to various risks, including stress on energy infrastructure and disruptions in energy supply systems.

Previous studies conducted by Il'yashenko *et al.,* [3] and Pioro and Pioro [4] have reported that the most rational heat recovery scheme using WHBs is to obtain steam using energy parameters. In this case, the heat energy of waste gases is maximally used owing to its transformation into electrical or mechanical energy, with the simultaneous production of steam based on technological parameters or hot water for industrial and municipal consumers.

Previously we designed and patented a sectional thermosiphon WHB for cogeneration power plants [5]. The organization of natural circulation facilitates the enhancement of the operational reliability of the evaporator circuit, reduces capital costs, and decreases the costs of driving,

* *Corresponding author.*
E-mail address: iurii.dolganov@uni.lu

https://doi.org/10.37934/arfmts.112.1.139154

maintaining, and repairing the circulation pump. However, the occurrence of natural circulation in the evaporator circuits of thermosiphon WHBs has not been sufficiently studied. The methods used for determining the velocity and multiplicity of circulation do not consider the actual processes, and no criteria exist for the necessary and sufficient conditions to enable the directed movement of the medium in the circuit.

This study focused on the process of natural circulation in the evaporation circuits of sectional thermosiphon WHBs and methods to ensure their stability. The findings were obtained using a model based on ranked variables of velocity and heat flux densities in the evaporator. This can form the basis for improving the performance of thermosiphon WHBs in real-time applications.

1.2 Literature Review

Several types of thermosiphon steam boiler designs have been described in the literature. A study of Pioro *et al.,* [2] reported the design and general view of a boiler for producing superheated steam and proposed a unified section of a thermosiphon boiler. Ryzhkov *et al.,* [6] reported the design of a marine WHB with a combined heating surface to produce saturated steam and hot air. Furthermore, a boiler with combined heating on exhaust gases, using its own combustion chamber, and a thermosiphon heating surface was proposed by Dolganov *et al.,* [7]. A waste heat recovery solution based on a heat pipe heat exchanger for the aluminum die-casting industry is shown in the study by Jouhara *et al.,* [8].

The details of the thermosiphon WHB for a cogeneration power plant based on a gas turbine of 6700 kW (Figure 1) were reported by Epifanov *et al.,* [9] and in the utility model Patent of Ukraine [10].

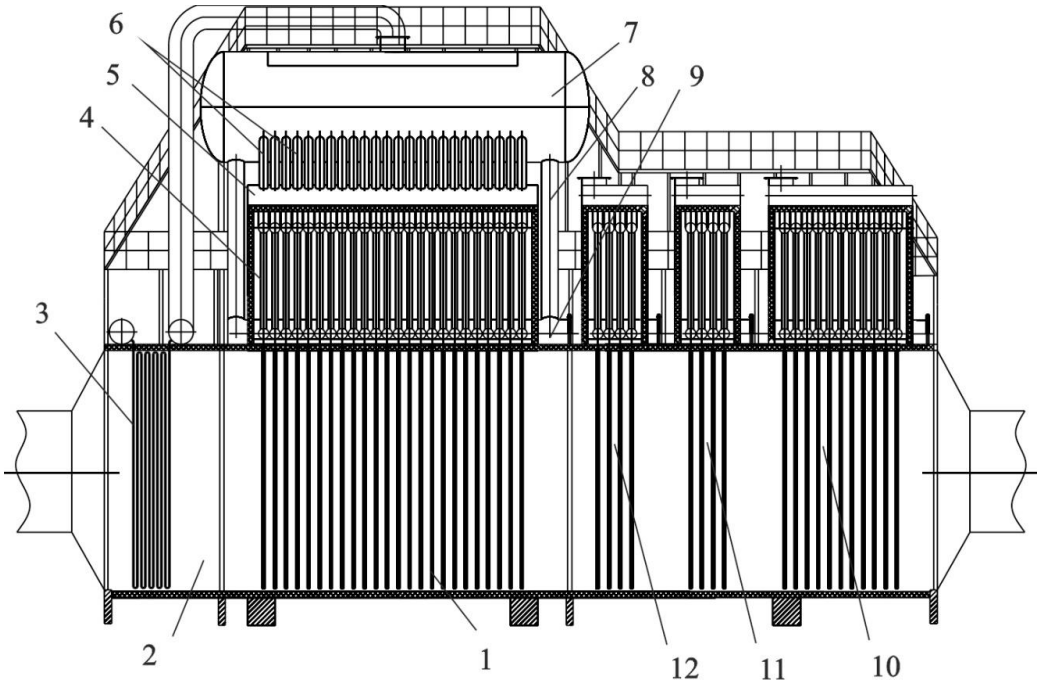

Fig. 1. Thermosiphon (WHB) for a cogeneration power plant: 1 – thermosiphon evaporator; 2 – gas duct; 3 – superheater; 4 – evaporator riser pipes; 5 – steam collection pipes; 6 – steam outlet pipes; 7 – steam drum; 8 – downcomer pipes; 9 – feeder pipes; 10 – gas water heater for consumer; 11 – gas condensate heater; 12 – economizer

In traditional evaporators with a vertical arrangement of pipes, natural circulation occurs owing to the useful pressure in the circuit. The useful pressure in the evaporator is greater than zero, and the reliability of circulation in the distributors and collectors of the evaporator can be verified [11]. The driving pressure of the circulation is determined by the height of the circuit and the difference between the densities of water in the downcomers and the steam–water mixture in the risers [12].

The assessment of the reliability of natural circulation generally involves determining the primary pipe and testing for stagnation, overturning, and heat transfer crises within the pipe. The absence of stagnation and overturning can be confirmed if the following conditions are fulfilled:

Stagnation safety factor:

$$K_{stg} = S_{stg}/S_{usf} \geq 1.1 \quad (1)$$

Overturning safety factor:

$$K_{over} = S_{over}/S_{usf} > 1.1 \quad (2)$$

Here, S_{stg} denotes the stagnation pressure, S_{usf} indicates the useful pressure, and S_{over} represents the overturning pressure.

Typically, the temperature regime of the evaporator pipe wall is determined using internal cooling conditions mentioned by Groeneveld *et al.,* [13]. The high intensity of heat transfer during boiling can be ensured by continuously wetting the inner surface of the wall with liquid. However, the contact between the wall and liquid phase may break under certain conditions, resulting in a sharp decrease in the heat transfer coefficient. This phenomenon is referred to as the heat transfer crisis [14].

The verification of heat transfer crisis involves determining the boundary conditions of the degraded heat transfer and the area of their existence, identifying the boundary vapor content during the first or second type crisis, and comparing it with the mass and volume vapor content in the tested section.

2. Methodology

2.1 Geometry and Initial Thermal Data

Figure 2 depicts the calculation model of the circulation circuit and the initial and boundary conditions. Table 1 lists the geometric parameters of the circuit, and Table 2 summarizes the data from the thermal calculations of the WHB evaporator mentioned in [5].

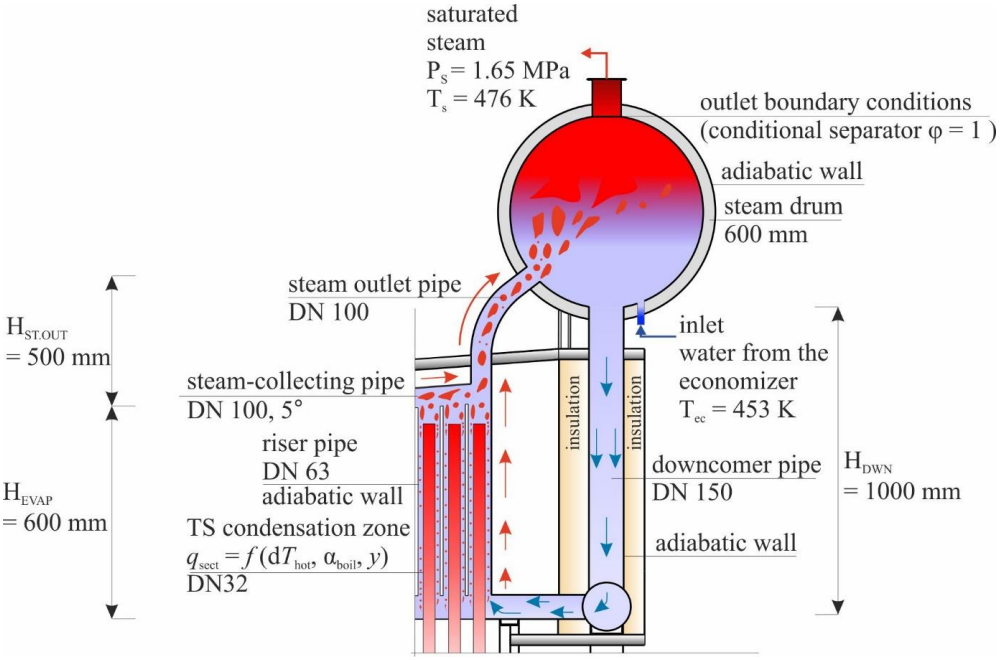

Fig. 2. Initial and boundary conditions of evaporation circuit (not to scale)

Table 1
Geometrical and thermal parameters of the circulation circuit

Parameter	Value
Steam pressure in the steam drum, MPa	1.65
Steam temperature in the separator, K	476
Inlet economizer water temperature, K	453
Number of sections	23
Number of thermosiphons per section	26
Diameter of the thermosiphon, m	0.032
Height of the condensation zone, m	0.55
Diameter of the riser pipe, m	0.063
Height of the riser pipe, м	0.6
Diameter of the downcomer pipe, m	0.15
Height of the downcomer pipe, m	1.0
Diameter of the steam outlet pipe, m	0.1
Height of the steam outlet pipe, m	0.5
Diameter of the steam outlet collection pipe, m	0.1
Inclination of the steam outlet collection pipe, °	5

Table 2
Thermal parameters of the evaporation surface obtained from the evaluation of the thermosiphon WHB for a cogeneration power plant with a gas turbine of 6700 kW

Section number	Heat flux, Q_{sect}, kW	Heat flux density, q_{sect}, kW/m^2	Average temperature of the thermosiphon condensation zone, T_{hot}, K
1	591.9	9.973	487.1
2	528.9	8.911	485.9
3	472.6	7.964	485.1
4	424.7	7.156	484.2
5	382.8	6.450	483.5
6	345.1	5.814	482.8
7	311.2	5.245	482.2
8	281.2	4.739	481.7
9	254.9	4.296	481.2
10	230.5	3.885	480.7
11	208.1	3.505	480.3
12	188.9	3.183	479.9
13	171.4	2.889	479.6
14	154.2	2.598	479.2
15	140.1	2.362	478.9
16	127.7	2.153	478.7
17	115.4	1.945	478.4
18	104.6	1.763	478.2
19	95.4	1.609	478.1
20	86.3	1.455	477.9
21	78.7	1.327	477.7
22	71.2	1.200	477.6
23	63.7	1.074	477.4

2.2 Analytical Solution

The solution to the classical hydraulic calculation problem of natural circulation in an evaporator is described in Baldina *et al.,* [11]. The primary task was to determine the velocity at the entrance to the riser pipes, assess the reliability of circulation in the circuit, and check for the absence of boiling crises in the annular channels of the evaporator tubes.

However, the classic solution does not fit the geometry of the presented circulation circuit with thermosyphons. The circulation velocity will change not only from section to section with a drop in the temperature of the flue gases, but also as they move away from the steam drum.

To obtain the hydraulic characteristics of the riser pipes, a ranked variable of the circulation velocity W_{circ} = 0.1, 0.2 … 5 m/s, and a function of the heat flux density $q_{sect} = f$ (dT_{hot}, α_{boil}, y) were introduced. Where dT_{hot} – temperature gradient on thermosiphon condensation zone (K), α_{boil} – heat transfer coefficient (W/m^{2}K), y – vertical coordinate (mm).

The heat transfer coefficient during boiling in the annular channel was determined using the following Isachenko empirical formula [15]:

$$\alpha_{boil} = 38.7 p_s^{0.5} \mathrm{d}T^{2.33} \quad (3)$$

where p_s is the saturation pressure (Pa).

With the riser movement of the steam–water mixture, the determining parameter was the value of φ, which denotes the volumetric steam content of the steam–water mixture flow. Here, the actual distribution of steam and water velocities in the pipe section was considered.

Average volumetric steam content in the riser pipes:

$$\varphi_{evap}(W_{circ}) = \frac{{}^{0.5D_{sect}(W_{circ})}/_{F_{evap}\rho''}}{W_{circ}+\left({}^{0.5D_{sect}(W_{circ})}/_{F_{evap}\rho''}\right)\left(1-\frac{\rho''}{\rho'}\right)} \quad (4)$$

Average volumetric steam content in the steam-collecting pipes:

$$\varphi_{st.out}(W_{circ}) = \frac{{}^{D_{sec}(W_{circ})}/_{F_{st.out}\rho''}}{W_{circ}+\left({}^{D_{sec}(W_{circ})}/_{F_{st.out}\rho''}\right)\left(1-\frac{\rho''}{\rho'}\right)} \quad (5)$$

Based on these values, the total pressure losses in the circuit were calculated as

$$S_{evap}(W_{circ}) = \left(10\varphi_{evap}(W_{circ}) \times H_{evap} \times (\rho' - \rho'')\right) - \sum \Delta P_{evap}(W_{circ}) \quad (6)$$

$$S_{st.out}(W_{circ}) = \left(10\varphi_{st.out}(W_{circ}) \times H_{st.out} \times (\rho' - \rho'')\right) - \sum \Delta P_{st.out}(W_{circ}) \quad (7)$$

$$S_{circ}(W_{circ}) = S_{evap}(W_{circ}) + S_{st.out}(W_{circ}) \quad (8)$$

The total resistance of the downcomer pipes was calculated using

$$\Delta P_{dwn}(W_{circ}) = (\lambda_0 H_{dwn} + \sum \xi_{dwn}) W_{dwn}^2 \frac{\rho'}{2} \quad (9)$$

In these equations, D_{sect} – section steam capacity (kg/s), F_{evap}– evaporator surface area (m^2), $F_{st.out}$ – steam outlet pipes surface area (m^2), ρ' – water density (kg/m^3), ρ'' – steam density (kg/m^3), H_{evap} – evaporator height (m), $H_{st.out}$ – steam outlet pipes height (m), H_{dwn}– downcomer pipe height (m), ΔP_{evap} – pressure loss in evaporator (Pa), $\Delta P_{st.out}$– pressure loss in steam outlet pipes (Pa), λ_0 – reduced friction coefficient, ξ – total coefficient of local resistance, φ_{evap} – steam volume fraction in evaporator, $\varphi_{st.out}$– steam volume fraction in steam outlet pipes, W_{dwn}– velocity in downcomer pipes (m/s).

Analytically, the point of intersection of the total useful pressure curve and the total resistance of the downcomer pipes were determined. Based on this, the actual flow rates and the average circulation velocity of the sections were evaluated. The Mathcad Prime package (version 7.0) was used to describe the algorithm and analytically determine the point of actual circulation velocity.

$$W_a = W_{circ\_min}, W_b = W_{circ\_max} \quad (10)$$

$$f(W_{circ}) = S_{circ}(W_{circ}) - \Delta P_{st.out}(W_{circ}) \quad (11)$$

$$W'_{circ} = root(f(W_{circ}), W_{circ}, W_a, W_b) \quad (12)$$

2.3 Numerical Simulation

The results obtained from the analytical model were averaged and could not completely characterize the processes in the circuit or localize the locations with boiling crises, circulation stagnation, and overturning. Various numerical simulation methods have been used to verify the analytical solutions with high accuracy [16]. Using the recommendations provided by Boyd [17], the physical geometry was represented with a finite-volume mesh, based on which the governing Navier–Stokes equations were discretized and solved. All models were developed using Ansys Fluent 2022 R2.

2.3.1 Physical model

The specific features of the computational fluid dynamics (CFD) model and major assumptions are outlined below and summarized in Table 3.

As the solutions were expected to be unsteady, a transient solver was applied under steady boundary conditions. The Eulerian volume of fluid model with the Lee model of evaporation–condensation phase interaction was used to simulate a two-phase flow. The flow in the annular channels was a stratified flow of immiscible media with a distinctly extended interface; in other words, the flow was comparable in size to that of the computational domain [18]. A single set of momentum conservation equations was solved for all phases, along with the equations for the transfer of the volume fraction of each phase. The model considered the influence of gravity. A standard k-epsilon turbulence model with enhanced wall treatment, thermal effect, and curvature correction was used. The “Real Fluid” functions of water and steam were added to the model, which included the following: thermodynamic properties; transport properties; saturation properties; spinodal curves. The saturated steam outlet was set as the opening condition, and the liquid/vapor phase in the air outlet section was analyzed.

In this paper, CFD model of evaporation circuit based on VOF method was used. Because there are only steam-liquid two phases in the flow field of WHB evaporation circuit, the sum of volume fractions for the two phases is always equal to unity $\alpha_l + \alpha_{st} = 1$. α_l is the volume fraction of liquid and α_{st} is the volume fraction of steam. And each cell in the domain is occupied by one phase or a combination of the two phases, the possible conditions of each phase are as follows:

$\alpha_l = 1$: The cell is filled with liquid phase.
$\alpha_l = 0$: The cell is filled with steam phase.
$0 < \alpha_l < 1$: The cell is at the interface between the liquid and steam phases.

Table 3
Summary of the parameters in simulation

General		
Solver	Type	Pressure-Based
	Time	Transient
	Gravity	−9.81
Models		
Multiphase Model	Homogeneous model	Volume Of Fluid (VOF)
	Formulation	Explicit Courant Number <2
	Lee evaporation – condensation	Improved by "Real Fluid" functions
Energy	On	
Viscous model	k-epsilon with enhanced wall treatment, thermal effect, and curvature correction	
Solution Methods		
Pressure-velocity coupling	SIMPLE	
Spatial discretization	Pressure	PRESTO
	Volume Fraction	Geo-Reconstruct
	Momentum	First Order Upwind
Other Settings		
Convergence criterion	0.0001	
Time step	0.00001	

2.3.2 Mesh independence

Three different grid sizes, with 65.000, 85.000 and 105.000 (rounded figures) computational cells, are generated and evaluated to check the grid independency of the system. As a boiling crisis is formed near the hot wall, 10 mesh layers are used as the boundary layer to capture all changes near the hot wall (TS condensation zone).

The average temperature of the thermosiphon condensation zone for first four sections are shown in Table 4. A slight difference can be seen in the prediction of the hot wall temperature between the 65.000 and 105.000 computational cells. Therefore, to reduce the calculation costs, the grid size with 85.000 cells is selected in the simulation.

Table 4
The results of the grid independency for validation part

Mesh Size (Cells)		65.000	85.000	105.000
Average temperature of the thermosiphon condensation zone, T_{hot}, K	1 section	486.2	487.0	487.4
	2 section	486.0	486.0	486.2
	3 section	484.6	484.8	485.1
	4 section	483.6	484.2	484.3

For properly modeling turbulent viscous flows in the near-wall region using CFD, it is necessary that the first cell height (height of the first row of cells near the wall) the mesh/grid should be according to the Y+ resolution required by the turbulence model. Y+ is a dimensionless parameter in fluid dynamics, defined as the dimensionless distance from the wall, generally used to express height relative to the viscous sub-layer near the wall.

To determine the height of the first cell Churchill equation (13) to (16) (which is valid for all flow regimes) for internal flows was used [19]. For turbulence models k-epsilon with Enhanced Wall Treatment Y+ should be equal to 1. The results are shown in Table 5.

Friction factor [19]:

$$F = 8 \cdot \left[\left(\frac{8}{Re} \right)^{12} + \frac{1}{(B+C)^{1.5}} \right]^{1/12} \tag{13}$$

where

$$B = \left[2.457 \ln \frac{1}{\left(\frac{7}{Re} \right)^{0.9} + \left(\frac{0.27\varepsilon}{H_{evap}} \right)} \right]^{16} ; C = \left(\frac{37530}{Re} \right)^{16} \tag{14}$$

First cell height for Fluent use

$$d_s = \frac{2Y^+ \mu_{dyn}}{U_F \rho} \tag{15}$$

where

$$T = \frac{F \rho {W_{circ}}^2}{2} \; U_F = \left(\frac{T}{\rho} \right)^{0.5} \tag{16}$$

Table 5
The results of the first cell height calculation

Density, ρ kg/m^3	Dynamic viscosity, μ_{dyn} kg/(m·s)	Velocity, W_{circ} m/s	Reference length, H_{evap}, m	Desired value for Y^+	Reynolds Number	First cell height, d_s, m
861.3	$1.32 \cdot 10^{-4}$	1.858	0.6	1	$6.05 \cdot 10^6$	$4.997 \cdot 10^{-6}$

2.3.3 Navier-Stokes equations

Continuity equation

For the VOF model, the liquid-vapor interface can be traced by solving the continuity equation of liquid volume fraction, it can be written as [20]:

$$\frac{\partial}{\partial t} (\alpha_l \rho_l) + \nabla \cdot (\alpha_l \rho_l \overrightarrow{u_l}) = S_M \tag{17}$$

where α_l, ρ_l , $\overrightarrow{u_l}$ represent the volume fraction, density, and velocity vector of the liquid phase, respectively; S_M is mass source term used to calculate the mass transfer during evaporation.

Momentum equation

Single momentum equation is solved throughout the domain, and the resulting velocity field is shared among the phases. The momentum equation, shown below, is dependent on the volume fractions of all phases through the properties volume-averaged density ρ and volume-averaged dynamic viscosity μ [20]:

$$\frac{\partial}{\partial t} (\rho \vec{u}) + \nabla \cdot (\rho \vec{u} \vec{u}) = -\nabla P + \nabla \cdot \left[\mu \left(\nabla \vec{u} + \nabla \overrightarrow{u^T} \right) \right] + \rho \vec{g} + \vec{F} \tag{18}$$

$$\mu = \alpha_l \mu_l + \alpha_{st} \mu_{st} \quad (19)$$

$$\rho = \alpha_l \rho_l + \alpha_{st} \rho_{st} \quad (20)$$

where $\vec{g}$ is the acceleration of gravity, P is the pressure, $\vec{F}$ is the external force acting on the fluid.

In addition, a surface tension model has been added to the model, improved by using "Real Fluid" functions: the dependence of the surface tension of water and steam on temperature and pressure.

Energy equation

The energy equation for the case of two-phase fluid circulation is shown below [20]:

$$\frac{\partial}{\partial t}(\rho E) + \nabla \cdot ([\vec{u}(\rho E + P)]) = \nabla \cdot (\lambda \nabla T) + S_E \quad (21)$$

$$\lambda = \alpha_l \lambda_l + \alpha_{st} \lambda_{st} \quad (22)$$

where S_E is the energy source term contained contribution from evaporation in circuit, and volume-averaged thermal conductivity λ.

The VOF model treats energy, E, and temperature, T, as mass-averaged variables:

$$E = \frac{\alpha_l \rho_l E_l + \alpha_{st} \rho_{st} E_{st}}{\alpha_l \rho_l + \alpha_{st} \rho_{st}} \quad (23)$$

where E_l , E_{st} are the energy for liquid and steam phase, respectively.

Turbulence model

The two-equation Renormalization Group (RNG) k − ε model was used in this study following the recommendation of the work by Sakr *et al.,* [21]. The most general multiphase turbulence model solves a set of k and ε transport equations for each phase. This turbulence model is the appropriate choice when the turbulence transfer among the phases plays a dominant role:

$$\frac{\partial}{\partial t}(\rho k) + \frac{\partial}{\partial x_i}(\rho k u_i) = \frac{\partial}{\partial x_j}\left(\alpha_k \mu_{eff} \frac{\partial k}{\partial x_j}\right) + G_k + G_b - \rho\varepsilon - Y_M + S_k \quad (24)$$

$$\frac{\partial}{\partial t}(\rho \varepsilon) + \frac{\partial}{\partial x_i}(\rho \varepsilon u_i) = \frac{\partial}{\partial x_j}\left(\alpha_\varepsilon \mu_{eff} \frac{\partial \varepsilon}{\partial x_j}\right) + C_{1\varepsilon} \frac{\varepsilon}{k}(G_k + C_{3\varepsilon} G_b) - C_{2\varepsilon} \rho \frac{\varepsilon^2}{k} - R_\varepsilon + S_\varepsilon \quad (25)$$

$$\mu_{eff} = \mu + C_\mu \rho \frac{k^2}{\varepsilon} \quad (26)$$

where S_k and S_ε are the additional source terms, G_k represents the production of turbulence kinetic energy caused by the mean velocity gradients, G_b represents the generation of turbulence kinetic energy due to buoyancy, Y_M represents the contribution of the fluctuating dilatation in turbulence to the overall dissipation rate, constants C_μ = 0.0845, $C_{1\varepsilon}$ = 1.42, $C_{2\varepsilon}$ = 1.68, respectively, μ_{eff} - the turbulent viscosity.

2.3.4 Phase change model

The Lee evaporation-condensation model is a mechanistic model, with a physical basis which described by Lee [22]. The mass transfer rates for boiling and condensation of Lee model are listed below:

$$\dot{m}_{l\to st} = coeff\,\alpha_l\rho_l\,\frac{T-T_{sat}}{T_{sat}} \text{ for evaporation process } (T > T_{sat}) \quad (27)$$

$$m_{l\to st} = coeff\,\alpha_{st}\rho_{st}\,\frac{T-T_{sat}}{T_{sat}} \text{ for condensation process } (T < T_{sat}) \quad (28)$$

However, the saturation temperature $T_{sat}$is specified as a constant in the Lee model. In the real working process of circulation in the WHB evaporator, the saturation temperature changes with pressure. If the influence of pressure on T_{sat} and the thermophysical properties of the liquid is not considered, then the Lee model cannot accurately predict the processes in the circulation loop. To solve this problem, Real Gas Properties (RGP) tables for water and steam were added to the developed model. RGP tables includes: thermodynamic properties (density, heat capacity, enthalpy, entropy, speed of sound); transport properties (viscosity, thermal conductivity); saturation properties (vapor pressure, boiling temperature, surface tension coefficient); spinodal curves.

3. Results

To examine the initiation of the steam formation and the possibility of natural circulation, the operational mode of the boiler was evaluated during start-up from a cold state for the most loaded section, namely the first section in the direction of gases. The disturbing influence of the evaporator dynamic model was the condensation zone temperature of the thermosiphons. Until the stationary mode was reached, the evaporator operated in the economizer mode, which was evident from the zero-vapor content at the evaporator outlet; the outlet boundary condition restricted the outlet of the mixture until the specified temperature in the drum was reached, thereby simulating the actuation of the shut-off and control valves as a secondary disturbing action.

After the set parameters were reached in the steam drum, the boundary condition for the steam output was triggered, water from the economizer that was not heated to a boiling temperature continued to feed the circuit, and the system entered a steady state. Figure 3 illustrates the velocity vectors of the coolant in the circuit. Nine defining points were selected on the streamline for a quantitative comparison of the analytical and numerical modeling data.

The simulation provided a complete representation of the distribution of velocities over elements and sections, whereas the analytical solution provided the average phase velocity at a point or contour element. The analysis of the velocity vectors unambiguously confirmed the presence of natural circulation in the evaporator and facilitated the quantitative determination of the average and local circulation velocities in each circuit element.

The graph of the velocity distribution over time (Figure 4) was conditionally divided into two regimes, namely, start-up and stationary modes. The transition from one regime to another was characterized by the stabilization of pulsations within the velocities of the steam and water fractions in the evaporation and downcomer pipes.

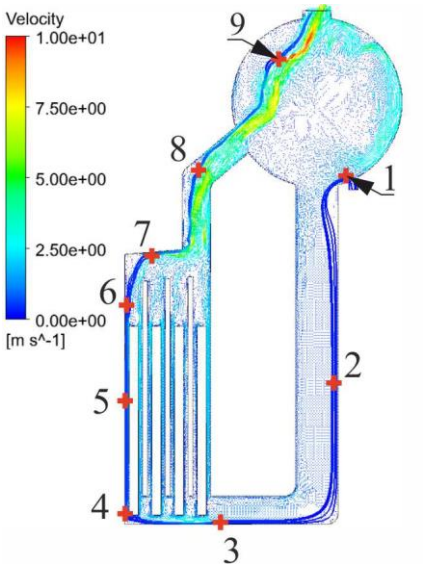

Fig. 3. Mixture velocity vectors with defining points on the streamline

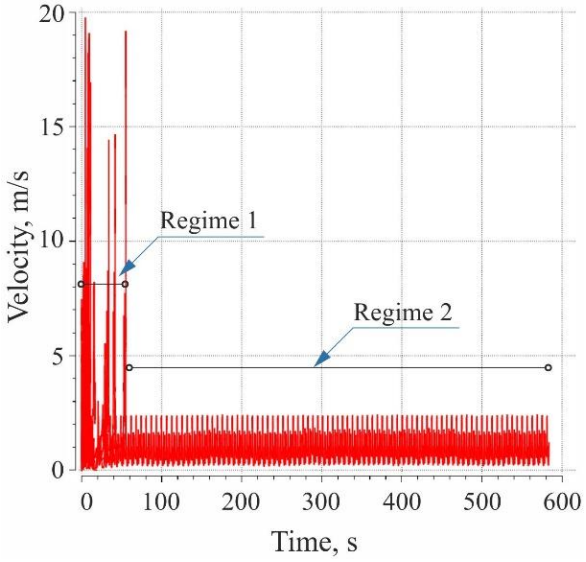

Fig. 4. Velocity value as a function of time

For convenience in determining the local parameters, a streamline of one complete circulation was introduced into the simulation results from the point of the water inlet of the economizer to the steam outlet (Figure 5). This was passed through the fourth evaporator tube because the flow was not stabilized in the initial three evaporator tubes.

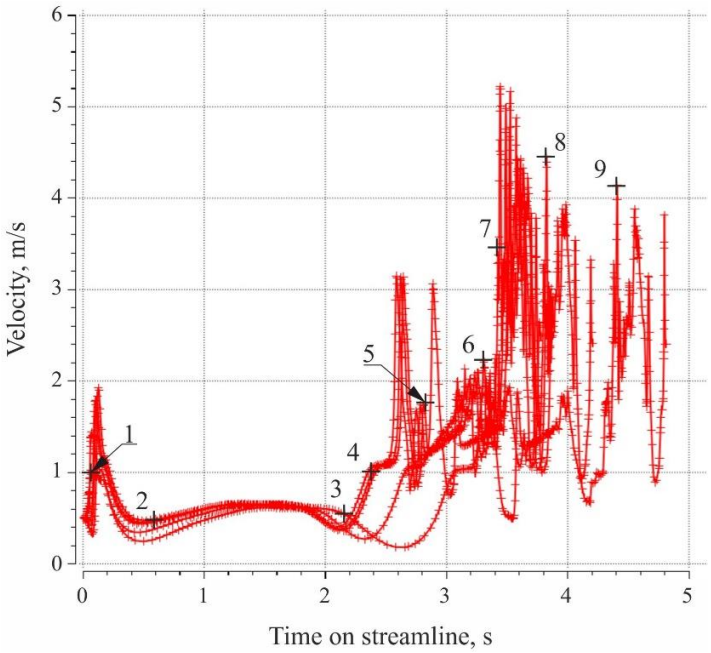

Fig. 5. Velocity value as a function of time on the streamline

To obtain an approximate estimate of the possibility of a heat transfer crisis, the degraded heat transfer limit was calculated in accordance with the recommendations for vertical steam-generating pipes and compared with the simulation results [11]. The boundary steam content, where a second-order heat transfer crisis occurred, was $\varphi_{crit} = 67.5\%$, which was substantially higher than the steam content at the outlet of the most heat-stressed evaporator tube (the first section along the gas flow) $\varphi_{st.out} = 58.44\%$ (point 6 on the streamline, Figure 6).

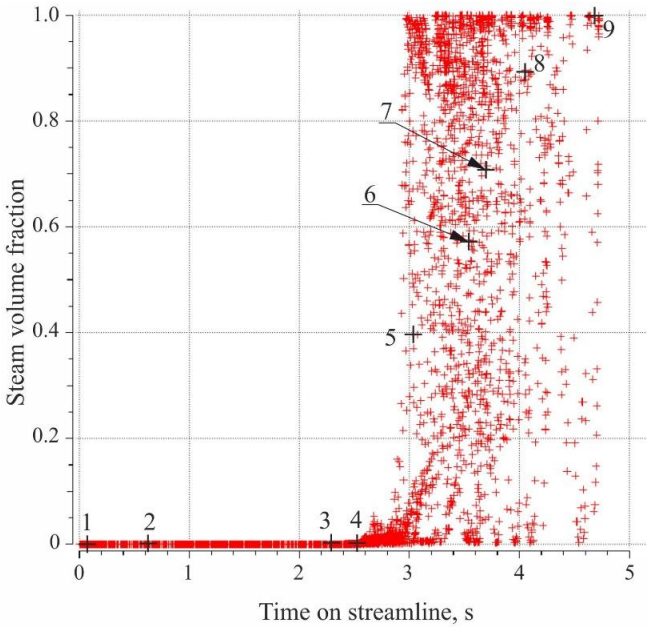

Fig. 6. Steam volume fraction value as a function of time on the streamline

The comparative results exhibited adequate convergence at the defining points, where the analytical model facilitated the calculation of velocity and volumetric steam content (Table 6). The relative error was calculated:

$$\left(\frac{W_{circ}^{A}-W_{circ}^{CFD}}{W_{circ}^{A}}\right)\times 100\% \quad (29)$$

Table 6
Flow parameters in the defining points

Control point	Variable	CFD	Analytical	Relative error (%)
1. inlet economizer water	Water velocity, m/s	1.000	1.000	-
	Volumetric steam content, %	0	0	-
2. downstream pipe	Water velocity, m/s	0.472	0.459	2.83
	Volumetric steam content, %	0	0	-
3. downstream pipe	Water velocity, m/s	0.501	0.459	9.15
	Volumetric steam content, %	0	0	-
4. inlet to evaporation pipes	Water velocity, m/s	1.033	1.000	3.3
	Volumetric steam content, %	0	0	-
5. evaporation pipes	Average mixture velocity, m/s	1.831	1.858	1.453
	Average volumetric steam content, %	39.12	40.0	2.2
6. outlet from evaporation pipes	Average mixture velocity, m/s	2.271	2.375	4.379
	Average volumetric steam content, %	58.44	57.11	2.329
7. steam-collecting pipes	Average mixture velocity, m/s	3.536	3.375	4.77
	Average volumetric steam content, %	70.18	70.0	0.26
8. steam outlet pipes	Average mixture velocity, m/s	4.441	4.568	2.78
	Average volumetric steam content, %	87	-	-
9. steam outlet	Outlet steam velocity	4.123	-	-
	Volumetric steam content, %	1	1	-

In the annular steam-generating channel, the steam content continuously increased along the length owing to the supply of heat, which in turn increased the speed of the mixture. However, an increase in the water velocity and the mass flow rate at the inlet of the evaporation channel decreased the vapor fraction in the mixture, improved the heat transfer, and reduced the likelihood of boiling crises. At certain points, complete evaporation of the liquid occurred with $\varphi_{evap} = 1$ or complete filling with water occurred ($\varphi_{evap} = 0$). Mixture velocities greater than 5 m/s indicated $\varphi_{evap} \to 0$. However, as the circulation velocity in the steam-generating channel was the actual velocity at which a single-phase liquid was supplied to the inlet, the vapor content was determined only at the outlet of the heating zone to identify the heat transfer crises in the hot zone of the thermosiphon.

4. Conclusion

This study entailed an analysis of the possibility of organising the natural circulation in a complex circuit of a thermosiphon WHB evaporator surface. In the analysed range of heat flux densities q_{sect} = 1.074–9.973 kW/m^2 and temperatures of the hot zone of thermosiphons T_{hot} = 477.4–487.1 K, no overturns and circulation stagnations were observed. The circulation rate was 0,459 m/s in downcomers till 4,568 m/s in steam outlet pipes which corresponds to generally accepted standards for the steam boilers design. The highest volumetric vapor content was $\varphi_{st.out} = 58.44\%$ and did not exceed the critical values $\varphi_{crit} = 67.5\%$. Thus far, the experimental verification of the data obtained from the circulation velocity in the thermosiphon WHB evaporator surface based on CFD and an analytical model has not been performed. However, the proposed analytical solution for determining the velocity in the elements of the circulation circuit exhibited adequate convergence and concurred with the data published in the existing literature. Therefore, it can be used for engineering calculations in the design of steam thermosyphon boilers for heat recovery systems in cogeneration power plants and heat recovery systems in offshore power plants.

The main scientific novelty of this work is the methodology used to obtain circulation rates and steam content patterns in complex circulation circuits of thermosiphon steam boilers. The developed model differs from the classical solution in that, using a ranked variable, it allows one to calculate the circulation rate not only for sections of the boiler, but also for each riser pipe separately. Using a ranked variable velocity to obtain the hydraulic characteristics of the evaporator tubes and determine the steam content inside and outside the heating zone simplified the tests for boiling and circulation crises. Furthermore, the mass flow rates were quantified based on boiler sections. Thus, the study findings can aid the development of enhanced thermosiphon WHBs.

The main limitation of this study is that the WHB is designed for a cogeneration power plant with a 6700 kW gas turbine; however, the capacity of such boilers is much wider. Therefore, the range of thermal loads, temperature, and saturation steam pressure must be increased.

In the future, the experimental setup will be improved to ensure the high accuracy and reliability of the findings. The authors intend to continue analysing the issue of natural circulation in steam boilers by modifying the two-dimensional code into a three-dimensional one, thus increasing the range of thermal loads and saturation steam pressure, and introducing refined geometries of the steam drum, different pipe pitches, diameters of thermosiphons, and annular evaporation channels into the model.

Disclosure statement

No potential conflict of interest was reported by the authors.

Data availability statement

The data that support the findings of this study, and software that implements the resulting model are available from the corresponding author, I. Dolganov, upon reasonable request.

Acknowledgments

The authors sincerely thank Professor Boris Dymo, Head of the Department of Thermal Physics, National University of Shipbuilding, Ukraine, for providing technical inputs and expert evaluation of the results. This research was not funded by any grant.

CRediT authorship contribution statement

Iurii Dolganov: Writing – original draft, Writing – review & editing, Conceptualization, Investigation, Software. **Alexander Epifanov**: Methodology, Supervision, Project administration. **Bohdan Lychko**: Formal analysis, Data curation.

References

[1] Reay, David, Ryan McGlen, and Peter Kew. *Heat pipes: theory, design and applications*. Butterworth-Heinemann, 2013.
[2] Pioro, I. P., V. A. Antonenko, and L. Pioro. *Efficient heat exchangers with two-phase thermosiphons*. Naukova Dumka, Kiev, 1991.
[3] Il'yashenko, I. S., O. N. Popov, and I. B. Smulyanskii. "Operation of waste heat boilers behind glass furnaces." *Glass and Ceramics* 1 (1986): 4-5.
[4] Pioro, L., and I. Pioro. *Two-Phase Thermosiphons and Their Industrial Applications*. Naukova Dumka, Kiev, 1988.
[5] Dolganov, I. "Increasing the efficiency of heat recovery of cogeneration gas-steam turbine plants with thermosyphon waste heat boilers." *PhD diss., Department of Thermal Physics, NUOS, Mykolaiv, Ukraine*, 2015.
[6] Ryzhkov, Sergey Vasilievich, Boris Vasilievich Dymo, and Alexander Anatolyevich Epifanov. *Steam generator*. USSR Patent 1451438, 1989.
[7] Dolganov, Iurii, Alexander Anatolyevich Epifanov, and Boris Vasilievich Dymo. *Combined waste heat boiler*. Ukraine Patent UA 82747, 2013.
[8] Jouhara, Hussam, Nerea Nieto, Bakartxo Egilegor, Josu Zuazua, Eva González, Ignacio Yebra, Alfredo Igesias et al. "Waste heat recovery solution based on a heat pipe heat exchanger for the aluminium die casting industry." *Energy* 266 (2023): 126459. https://doi.org/10.1016/j.energy.2022.126459
[9] Epifanov, Alexander Anatolyevich, Boris Vasilievich Dymo, Iurii Dolganov, and Natalia O. Melnychuk. "Features of design and methods of thermal calculation of thermosiphon sectional waste heat boiler." *Collection of Scientific Papers of NUS* 2 (2011): 97-105.
[10] Dolganov, Iurii, Alexander Anatolyevich Epifanov, and Boris Vasilievich Dymo. *Thermosiphon waste heat boiler*. Ukraine Patent UA 97905, 2015.
[11] Baldina, O. M., V. A. Lokschin, D. F. Peterson, I. E. Semenovker, and A. L. Schvarc. "Hydraulic calculation of boiler plants-The Normative method." *Energia, Moscow* (1978).
[12] Walter, Heimo, Wladimir Linzer, and Thomas Schmid. "Dynamic flow instability of natural circulation heat recovery steam generators." In *ISTP-16, The 16th International Symposium on Transport Phenomena*, p. 11. 2005.
[13] Groeneveld, D. C., A. Ireland, J. Kaizer, and A. Vasic. "An overview of measurements, data compilations and prediction methods for the critical heat flux in water-cooled tubes." *Nuclear Engineering and Design* 331 (2018): 211-221. https://doi.org/10.1016/j.nucengdes.2018.02.031
[14] Kutateladze, Samson Semenovich, and Mikhail Adol'fovich Styrikovich. *Hydraulics of gas-liquid systems*. Wright-Patterson Air Force Base, Ohio, 1976.
[15] Isachenko, V. P., V. A.Osipova, and A. S. Sukomel. "Heat transfer/Isachenko VP, Osipova VA, Sukomel AS." *Textbook for High Schools, Izd. 3rd revision., Add.-Moscow: Energia* 488 (1975).
[16] Peng, Dong, Xu Yanying, and Lan Rihua. "Loop Analysis Method for the Numerical Calculation of Hydrodynamic Characteristic of Boiler with Natural Circulation." *Journal of Harbin Institute of Technology* 39, no. 3 (2007): 462-466.
[17] Boyd, Christopher. *CFD Predictions of Severe Accident Natural Circulation Flows in a Combustion Engineering PWR*. American Nuclear Society-ANS, Thermal Hydraulics Division, 555 North Kensington Avenue, La Grange Park, IL 60526 (United States), 2016.

[18] Habib, Mohamed A., H. E. Emara-Shabaik, and I. Al-Zaharnah. "Numerical investigation of thermal and physical characteristics of circulating flow in boiler risers using a nonlinear dynamic model." *Computational Thermal Sciences: An International Journal* 2, no. 1 (2010). https://doi.org/10.1615/ComputThermalScien.v2.i1.10
[19] Churchill, Stuart W. "Friction Factor Equations Spans All Fluid-Flow Regimes." *Chemical Engineering Journal* 84 (1977): 91-92.
[20] ANSYS Fluent. "ANSYS Fluent Theory Guide, ANSYS." *ANSYS Inc., Release 15, Canonsburg, PA, USA* (2013).
[21] Sakr, I. M., W. A. El-Askary, Ashraf Elwy Balabel, and K. Ibrahim. "Computations of upward water/air fluid flow in vertical pipes." *CFD Letters* 4, no. 4 (2012): 193-213.
[22] Lee, W. H. "A pressure iteration scheme for two-phase flow modeling. Multiphase Transport Fundamentals, Reactor Safety, Applications." *Hemisphere Publishing, Washington, DC* (1980).